

OPTIMIZATION AND MODELING OF SILICON-GERMANIUM THIN FILM TRANSISTORS FOR AMLCD APPLICATIONS USING A PLACKETT-BURMAN EXPERIMENTAL DESIGN

V. Subramanian¹, K. Saraswat¹, H. Hovagimian², and J. Mehlhaff²
¹ Electrical Engineering Department, Stanford University, Stanford, CA
² Intevac RTP Systems, Rocklin, CA

INTRODUCTION

Thin film transistors (TFTs) are used as pixel transistors in active matrix liquid crystal displays (AMLCDs). Polycrystalline TFTs enable the inclusion of driver circuitry on the display substrate, and allow for higher quality displays¹. Glass substrates are necessary for large display panels, imposing an upper limit on process temperatures to minimize warpage. Solid phase crystallization² and laser annealing³ are two conventional means of crystallizing films for TFT channels. However, both suffer from low throughput. Scanned rapid thermal annealing (RTA) promises a high-throughput glass-compatible poly-TFT process⁴. Silicon-Germanium (SiGe) alloys are an alternative to conventional silicon films as they permit lower processing temperatures. The combination of scanned RTA and SiGe holds promise as a means of implementing a high-throughput poly-TFT process⁵.

The SiGe alloy system, being a binary system, has complex thermodynamic characteristics, and has not been fully characterized. The numerous interactions between process parameters make a full factorial experiment impractical. We describe the use of a Plackett-Burman⁶ multifactorial design to determine preliminary effects and interactions. The results obtained from this matrix have been used to develop an easily realizable response surface matrix for complete characterization of the system. This will allow the optimization of the TFT process.

EXPERIMENTAL DESIGN

Based on theoretical considerations, several parameters requiring study were identified. Characterizing the SiGe system requires a study of various deposition and crystallization parameters, such as deposition temperature and pressure, seed layer thickness, cleaning species, and scan speed during RTA. The temperature and pressure requirements have been extensively studied for silicon⁷. However, the binary nature of SiGe complicates the deposition process, and a study of the thermodynamics of deposition is necessary. Parameters such as seed layer thickness and RTA scan speed are unique to this technology and have never been studied in detail.

In order to reduce the size of the overall experimental space, a two stage approach was employed. Our approach makes use of a simple screening experiment with a more complex response surface design to follow. The screening experiment was designed to establish the relative importance of the various process parameters, and to assist in the identification of any of the important interactions. For the SiGe system, theoretical considerations suggest that interactions may be important. The confounding scheme for the interactions and main effects was therefore determined and documented as an integral part of the screening design experimental matrix. Finally, each factor within the screening experiment was restricted to two levels in order to minimize the number of treatment combinations while retaining the ability to identify interactions and grossly characterize the various process phenomena. Several parameters, such as the effect of Ge fraction, have already been individually studied previously, and were left out of the screening matrix. Any significant interactions involving these parameters will be studied later using another matrix.

Several responses of interest were defined. These responses are critical to fabricating high quality TFTs. They were carefully designated, and optimization goals were established. These are summarized in table I.

Table I: Response parameter definitions

<i>Response Parameter</i>	<i>Abbreviation</i>	<i>Unit</i>	<i>Definition</i>	<i>Target Condition</i>
Crystallization Temperature	T _{cryst}	°C	determined by ramping lamp power during scan to identify crystallization point	Minimize
Threshold Voltage	V _T	V	V _{GS} for which I _D =100nA(W/L); V _{DS} =10V	Minimize absolute
Leakage Current	I _{off}	pA/μm	I _D for V _{GS} =0V, V _{DS} = 10V	Minimize absolute
Linear Mobility	μ _{FE}	cm ² /V-sec	max. mobility for V _{GS} < 40V , V _{DS} = 0.1V	Maximize
Sub-Threshold Slope	sts	V/dec.	Inverse slope of I _D -V _G for V _{DS} = 10V , below V _T	Minimize absolute

Having established clearly defined optimization goals, a screening matrix for the first experiment was designed, using a standard 8 run Plackett-Burman orthogonal array. Five of the seven columns were assigned to the various experimental parameters of primary interest. Dummy variables were assigned to two of the contrast columns to identify critical interactions. The complete matrix definition is shown below, in table II.

Table II: Screening experiment design

	A	B	C	D	E	F	G
+	200mtorr	500°C		100Å	30sec	5mm/sec	
-	100mtorr	450°C		10Å	0sec	15mm/sec	
Run	Deposition Pressure	Deposition Temperature	Dummy	Seed Layer Thickness	Pre-deposition HF Dip	RTP Scan Speed	Dummy
1	-	-	-	-	-	-	-
2	-	-	-	+	+	+	+
3	-	+	+	+	+	-	-
4	-	+	+	-	-	+	+
5	+	+	-	-	+	+	-
6	+	+	-	+	-	-	+
7	+	-	+	+	-	+	-
8	+	-	+	-	+	-	+

The following confounding schemes are contained within the contrasts detailed above:

1. Contrast A = $E_{\text{dep. pressure}} - E_{\text{seed thickness}} \cdot E_{\text{HF predip}} + E_{\text{dep. temperature}} \cdot E_{\text{HF predip}} \cdot E_{\text{RTP scan speed}}$
2. Contrast B = $E_{\text{dep. temperature}} - E_{\text{seed thickness}} \cdot E_{\text{RTP scan speed}} + E_{\text{dep. pressure}} \cdot E_{\text{HF predip}} \cdot E_{\text{RTP scan speed}}$
3. Contrast C = $-E_{\text{dep. pressure}} \cdot E_{\text{dep. temperature}} - E_{\text{HF predip}} \cdot E_{\text{RTP scan speed}} + E_{\text{dep. pressure}} \cdot E_{\text{seed thickness}} \cdot E_{\text{RTP scan speed}} + E_{\text{dep. temperature}} \cdot E_{\text{seed thickness}} \cdot E_{\text{HF predip}}$
4. Contrast D = $E_{\text{seed thickness}} - E_{\text{dep. pressure}} \cdot E_{\text{HF predip}} - E_{\text{dep. temperature}} \cdot E_{\text{RTP scan speed}}$
5. Contrast E = $E_{\text{HF predip}} - E_{\text{dep. pressure}} \cdot E_{\text{seed thickness}} + E_{\text{dep. pressure}} \cdot E_{\text{dep. temperature}} \cdot E_{\text{RTP scan speed}}$
6. Contrast F = $E_{\text{RTP scan speed}} - E_{\text{dep. temperature}} \cdot E_{\text{seed thickness}} + E_{\text{dep. pressure}} \cdot E_{\text{dep. temperature}} \cdot E_{\text{HF predip}}$
7. Contrast G = $-E_{\text{dep. pressure}} \cdot E_{\text{RTP scan speed}} - E_{\text{dep. temperature}} \cdot E_{\text{HF predip}} + E_{\text{dep. pressure}} \cdot E_{\text{dep. temperature}} \cdot E_{\text{seed thickness}} + E_{\text{seed thickness}} \cdot E_{\text{HF predip}} \cdot E_{\text{RTP scan speed}}$

Since the relative magnitude of the confounded effects associated with a given contrast column generally follows the order of significance: primary effects \gg secondary interactions \gg tertiary interactions the identities of the important effects can be ascertained.

EXPERIMENTAL PROCEDURE

Devices were fabricated using a self-aligned top-gate TFT process. 1000Å SiO₂ was deposited on quartz wafers as a barrier layer. This is common to both quartz and glass processing. Hence, glass can be simulated with little deviation. LPCVD Si_{0.85}Ge_{0.15} was deposited for the channel and crystallized using a scanning RTA system, illustrated in figure 1. The film was patterned, and LTO gate oxide and an Si_{0.5}Ge_{0.5} gate electrode was deposited. The gates were patterned, and the devices were implanted, annealed, and passivated. Contacts were defined and Al/Si was used for metallization. Electrical measurements were made, and response parameters were extracted.

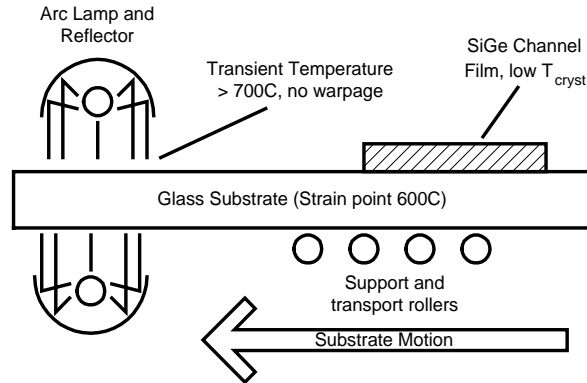


Figure 1: Cross section of RTA system.

RESULTS

The results obtained from the measurements performed on the devices made using the screening matrix are summarized below, in table III.

Table III: Response Matrix

#	Process Response	TFT Electrical Responses							
		NMOS				PMOS			
	T_{cryst}	V_T (V)	I_{off} (pA/ μ m)	μ_{FE} (cm ² /V-sec)	sts (V/dec.)	V_T (V)	I_{off} (pA/ μ m)	μ_{FE} (cm ² /V-sec)	sts (V/dec.)
1	836	22.9	4.425	0.812	3.8	-21.3	4.4	2.14	3.7
2	816	22.3	7.3	1.91	3.7	-21.1	5.25	4.64	3.6
3	797	17.2	2.045	2.32	3.2	-19.5	1.95	3.07	3.3
4	738	41*	0.477	0.0116	3.8	-40.5*	0.451	0.0174	4.2
5	760	13.8	1.03	5.22	2.6	-15.8	1.48	8.12	2.7
6	804	11.6	3.66	7.54	2.7	-15.4	2.2	12.8	2.6
7	815	20.7	5.2	1.74	3.7	-19.6	4.595	5.06	3.3
8	803	16.1	2.135	2.9	3.1	-18.1	2.91	5.8	3.1

The confounding scheme was extracted for each of the process factors and interactions up to the third order. The contrasts for the PMOS devices are illustrated in figures 2-6. NMOS devices exhibited similar contrasts.

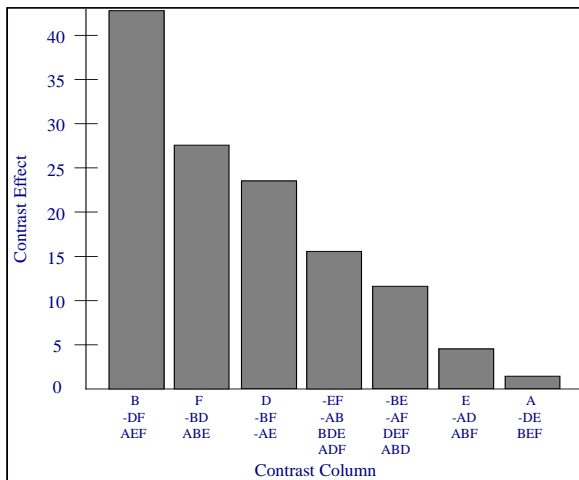


Figure 2: Crystallization temperature contrasts

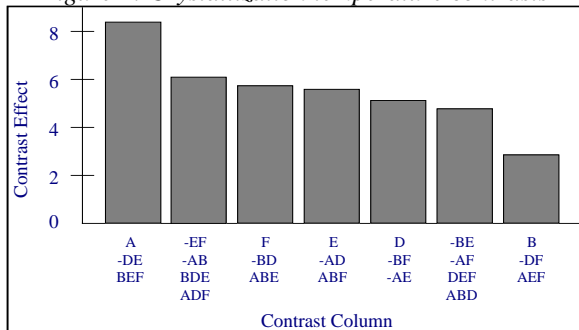


Figure 4: PMOS V_T contrasts

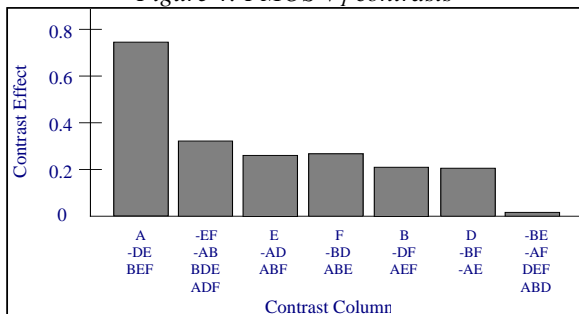


Figure 6: PMOS sub-threshold slope contrasts

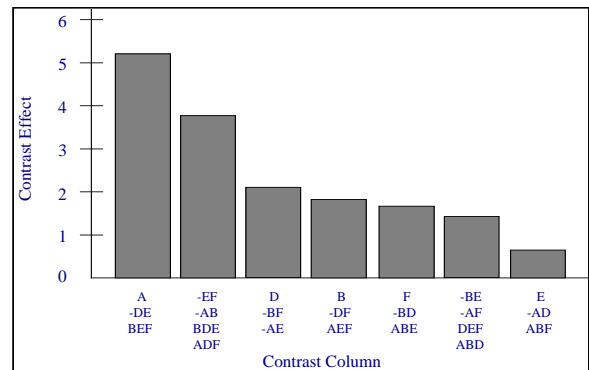


Figure 3: PMOS μ_{FE} contrasts

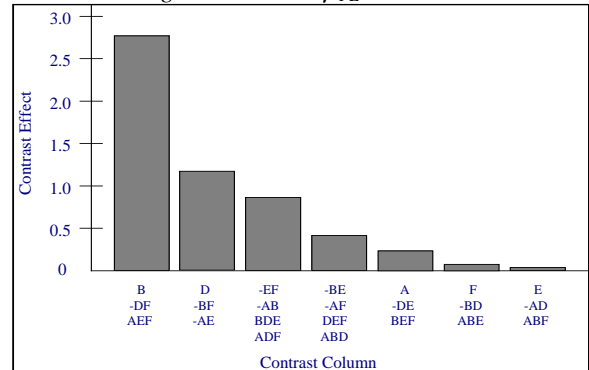


Figure 5: PMOS I_{off} contrasts

Figures 2-6 illustrate relative magnitudes of importance of various process parameters and confounded interactions. For any given contrast column: primary effects >> secondary interactions >> tertiary interactions.

Key	
A:	Deposition Pressure
B:	Deposition Temperature
C:	Dummy Variable
D:	Seed Layer Thickness
E:	Pre-deposition HF Dip
F:	RTP Scan Speed
G:	Dummy Variable

From the above figures, several conclusions can be drawn. Deposition pressure has a strong effect on most device parameters. Deposition temperature is the dominant contrast column affecting crystallization temperature, while the effect of pressure on the same is negligibly small. This gives us a highly useful optimization strategy for improving device performance without raising crystallization temperatures. The information obtained from this experiment has been utilized in the development of a response surface matrix, which will be used to model the system more completely. Several variables and interactions having minor contrasts have been eliminated, and the matrix has been expanded to enlarge the optimization windows. Initial results are extremely promising. Films deposited over a wide range of pressures have shown little change in crystallization requirement, while the crystalline quality, as determined by x-ray diffraction signatures, has improved substantially. This is illustrated in figure 7.

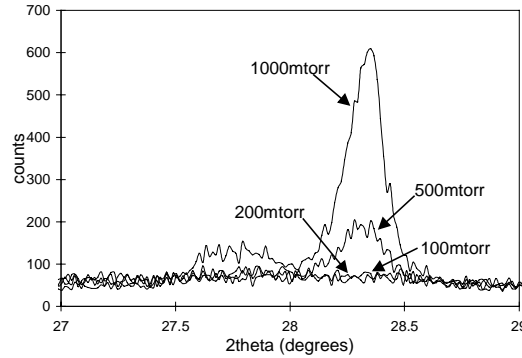


Figure 7: X-ray $\langle 111 \rangle$ peaks for films deposited at different pressures.

Clearly, the predictions made by the screening matrix appear to hold over a range of pressures substantially wider than the 2-level system used in screening.

CONCLUSIONS

The complexity of the SiGe system makes the use of a standard full factorial experimental design impractical. Instead, a two stage strategy of screening and response surface experimentation is being utilized to characterize the SiGe system for use in the development of a high throughput polycrystalline TFT technology for AMLCD applications. Stage I of this strategy consisted of a two level Plackett-Burman screening design developed and used to define dominant contrasts and interactions in the SiGe system. The information gleaned from the execution of this design has been used to develop optimization strategies for improving device performance and to provide input for the response surface. Preliminary confirmation experiments based on the information gleaned from the screening experiment show consistency with the results derived from the screening experiment. A response surface design will be used to better quantitatively understand these relationships.

ACKNOWLEDGEMENTS

This work was supported by the Advanced Research Projects Agency. The authors would like to thank Dr. T. King for her useful advice and assistance in device hydrogenation.

REFERENCES

1. I-W. Wu, Solid State Phenomena, **37-38** (1994) pp. 553-564
2. T. W. Little et al, Journal of the Society for Information Display, **1/2** (1993) pp. 203-209
3. D. H. Choi et al, Japanese Journal of Applied Physics, **33** (1994) pp. 83-86
4. J. Fair et al, International Flat Panel Display Conference SEMICON/West (1992) pp. A 109-112
5. S. Jurichich et al, Japanese Journal of Applied Physics, **33** (1994) pp. L1139-1141
6. R. L. Plackett et al, Biometrika, **33** (1946) pp. 305-325
7. A. I. Voutsas et al, Journal of the Electrochemical Society, **139** (1992) pp. 2659-2665